Journal of Marine Research, 50, 341–365, 1992

Journal of
MARINE RESEARCH

Volume 50, Number 3

A two-layer Gulf Stream over a continental slope

by Rick Salmon[1]

ABSTRACT

We consider the two-layer form of the planetary geostrophic equations, in which a simple Raylcigh friction replaces the inertia, on a western continental slope. In the frictionless limit, these equations can be written as characteristic equations in which the potential vorticities of the top and bottom layers play the role of Riemann invariants. The general solution is of two types. In the first type, the characteristics can cross, and friction is required to resolve the resulting shocks. In the second type, one of the two Riemann invariants is uniform, the remaining characteristic is a line of constant f/H, and the solutions take a simple explicit form. A solution resembling the Gulf Stream can be formed by combining three solutions of the second type. Compared to the corresponding solution for homogeneous fluid, the Gulf Stream and its seaward countercurrent are stronger, and the latter is concentrated in a thin frictional layer on the eastern edge of the Stream.

1. Introduction

Forty-four years have passed since Henry Stommel published the first correct theory of the Gulf Stream, but the theory of the Stream (and of ocean boundary currents in general) remains very incomplete. Despite many valuable contributions, there is as yet no completely deductive explanation of the cross-stream structure of the current, of its remarkable stability between the Florida Straits and Cape Hatteras, or of its sudden separation at the Cape. The earliest theories assumed that the ocean bottom was flat, or that the velocity vanished beneath the thermocline, and thus ignored the obvious fact that the Gulf Stream is controlled by the relatively steeply sloping seafloor beneath it, and not by the precise location of the coastline.

1. Scripps Institution of Oceanography, La Jolla, California 92093-0225, U.S.A.

However, the theory of baroclinic flow over sloping topography (to which the present paper offers a small contribution) has proved to be a considerable challenge.

Several earlier papers have considered analytic and numerical solutions to a particularly simple, inertia-less, set of model equations for large-scale ocean flow (Salmon, 1986, 1990; Salmon and Hollerbach, 1991).[2] These equations differ from the more exact primitive equations of ocean motion in that Rayleigh friction replaces the relative accelerations of fluid particles in all three directions. In nondimensional form, the equations are:

$$\begin{aligned} \mathbf{f} \times \mathbf{u} &= -\nabla\phi - \epsilon\mathbf{u} + \mathbf{f} \times \mathbf{u}_E \\ 0 &= -\phi_z + \theta - \epsilon\delta^2 w \\ u_x + v_y + w_z &= 0 \\ \theta_t + u\theta_x + v\theta_y + w\theta_z &= S + \kappa\nabla^2\theta. \end{aligned} \tag{1.1}$$

Here, $(u, v, w) \equiv (\mathbf{u}, w)$ is the velocity in the (eastward, northward, vertical) direction with coordinate (x, y, z); $\mathbf{f} = f\,\mathbf{k}$ where $f = y$ is the Coriolis parameter and $\mathbf{k}$ the vertical unit vector; ϕ is the pressure and θ the temperature (in the usual Boussinesq approximation). The prescribed vector $\mathbf{u}_E(x, y, z)$ is a horizontal body force that represents the input of wind momentum near the ocean surface. The diabatic heating, S, must generally include a convective adjustment at places of local static instability. The constants ϵ and $\epsilon\delta^2$ are coefficients of Rayleigh friction in the horizontal and vertical directions, respectively; κ is the diffusion coefficient for temperature.

Equations similar to (1.1) have been called the *planetary geostrophic equations,* a terminology we apply to (1.1). As shown in the previous papers, the planetary geostrophic equations, (1.1), are well-posed with respect to boundary conditions of no-normal flow and prescribed temperature (or temperature flux) at all boundaries. In interesting cases, ϵ, $\epsilon\delta^2$, and κ are all asymptotically small. Then the friction and diffusion terms are important only within thin *inner regions* located at the boundaries or in the ocean interior, where they were called *fronts.* The previous papers considered a rectangular ocean with a flat bottom and vertical sidewall boundaries at the coasts. In that geometry, the boundary layers include a western coastal boundary layer of thickness ϵ, northern and southern boundary layers of thickness $\epsilon^{1/2}$, and *upwelling layers* of thickness $\epsilon\delta$ at all vertical coastal boundaries. The upwelling layers, in which vertical friction is important and the motion is non-hydrostatic, exist wherever the Ekman flow $\mathbf{u}_E$ or the interior thermal wind has a component normal to the coastline. In the limit $\epsilon\delta^2 \to 0$ of vanishing vertical friction, these upwelling layers

2. Salmon and Hollerbach (1991) investigated the symmetry group of the thermocline equations, the Eqs. (1.1) with forcing and friction omitted, and stated that one particularly important member of that group ($\mathbf{v}_1$ in the notation of the paper) had "apparently not previously been noticed." I take this opportunity to note that this transformation had been previously discovered by Peter D. Killworth (1983), and I thank Dr. Killworth for bringing this to my attention.

become vanishingly small, but they can never disappear. That is, if vertical coastal boundaries are present, the solutions of (1.1) cannot be everywhere hydrostatic. However, if the ocean depth $H(x, y)$ goes smoothly to zero at the coastline, so that vertical boundaries are absent, then the limit $\epsilon\delta^2 \to 0$ in (1.1) is *regular:* The motion is globally hydrostatic and the upwelling layers entirely disappear. The more realistic geometry thus permits a slightly simpler dynamics.

With or without vertical sidewalls, the boundary-layer structure of the planetary geostrophic equations seems to be much simpler than the boundary-layer structure of the primitive equations with Fickian momentum diffusion ($\nabla^2\mathbf{u}$), where, typically, three nested boundary layers occur at coastal boundaries (e.g. Pedlosky 1968, 1969); and this simpler structure allows numerical solutions of the planetary geostrophic equations to probe the physically important limit of small friction and temperature diffusion to a greater degree than is currently possible with the physically richer, but mathematically much more complex primitive equations. The primitive equations *require* a momentum diffusion of at least Fickian order because the primitive horizontal momentum equations contain the advective term $\mathbf{u}\cdot\nabla\mathbf{u}$. In numerical solutions of the primitive equations, this advection produces progressively finer spatial scales of momentum, and diffusion of momentum is required to keep these scales within the limits of numerical resolution. However, the presence of so many required diffusion operators raises the differential order of the primitive equations as a whole. This leads to inner regions with complicated structure, and may require that the eddy coefficients be unrealistically large to maintain numerical stability: in numerical solutions of any system, the thinnest boundary layers (or fronts) must be resolved, or the solutions exhibit spurious behavior that typically includes oscillations on the scale of the grid-spacing. If, without understanding the very complex multiple-boundary-layer structure of the primitive equations, mixing coefficients are increased arbitrarily until the thinnest boundary layers are resolved, then the whole domain, and particularly the ocean interior, may be unrealistically diffusive. I believe that this—and not the more frequently mentioned presence of inertia-gravity waves—may be the biggest difficulty in using the primitive equations as the basis for numerical models. On the other hand, it seems always possible to choose the parameters in the planetary geostrophic equations (1.1) so that dissipative effects are confined to thin but fully resolved layers. Again, this is possible because of the low-order friction, and the low-order friction is sufficient only because momentum advection has been omitted. Fickian temperature diffusion, $\nabla^2\theta$, is required in (1.1d), because the temperature advection $\mathbf{u}\cdot\nabla\theta$ has been retained.

Of course, the idea that dissipation terms should take the simplest form consistent with the other terms in the dynamical equations rests on the tacit assumption that inner regions play an essentially passive role in the theory of ocean circulation. Moreover, the neglect of horizontal momentum may ultimately be unsatisfactory; the

inertia-less equations can probably not explain so important a feature as the huge recirculation of the Gulf Stream east of Cape Hatteras. However, I believe that the planetary geostrophic equations offer the best hope for physical understanding, and will explain far more of the general circulation than currently thought.

In this paper we consider a *two-layer* version of the planetary geostrophic equations in an ocean with realistic bottom relief. Our object is to understand the influence of topography and variable layer-thickness (baroclinicity) on boundary currents like the Gulf Stream. The two-layer model differs from the general planetary geostrophic equations (1.1) in the assumptions of

(a) global hydrostatic balance; and

(b) the existence of two immiscible fluid layers with different, constant temperatures.

We justify (a) by considering oceans with non-vertical sidewalls. The much more worrisome assumption (b) receives some support from the appearance of a front, with thickness $\kappa^{1/2}$, across which the temperature varies rapidly, in analytical and numerical solutions of the planetary geostrophic equations (Salmon, 1990; Salmon and Hollerbach, 1991). This front corresponds to the ocean's main thermocline. In the work reported here, the assumption (b) of two immiscible layers was nevertheless adopted with considerable reluctance, and only after repeated failures to construct a Gulf Stream theory based directly on (1.1). However, the two-layer solutions given below have interesting features that resemble the observed Gulf Stream.

Section 2 derives the two-layer equations in standard notation. In Section 3 we consider the relatively easy special case of a completely homogeneous ocean, emphasizing the striking difference between oceans of *infinite* northward extent and those with realistically *finite* horizontal dimensions. In the former, friction controls the width and location of both the Gulf Stream and the countercurrent induced by the continental slope. However, in oceans of finite extent, the Gulf Stream and countercurrent are steered by the topography and, in the limit of small friction, are locally independent of the friction. The reasoning in Section 3 (which, though probably unappreciated, is not new) may explain features of the flow along eastern North America, including the huge southward transport recently observed east of the Bahamas.

In Section 4, we show that the frictionless form of the general two-layer equations can be written as characteristic equations in which the potential vorticities of the top and bottom layers play the role of Riemann invariants. These equations can be completely solved, and the general solution is of two types. In the first type, the characteristics can cross, and friction is required to resolve the resulting shocks. The solutions can be written in implicit form. In the second type, one of the two Riemann invariants is uniform, the remaining characteristic is a line of f/H, and the solutions take a simple explicit form.

Section 5 analyzes a solution of this second type that resembles the Gulf Stream.

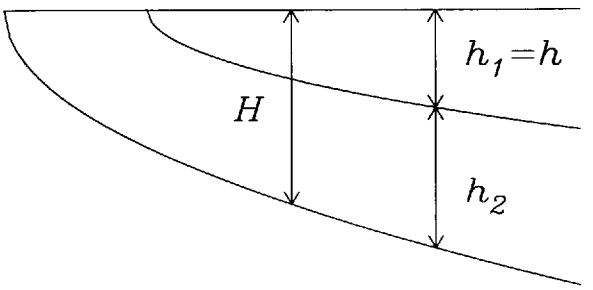

Figure 1. The two-layer model with surface outcrop.

The solution consists of three regions: an inshore region in which the upper-layer thickness vanishes, a Gulf Stream region in which the *lower*-layer potential vorticity is uniform, and an offshore region of uniform *upper*-layer potential vorticity. These regions are bounded by f/H-lines at which frictional inner regions occur. The effects of baroclinicity and relief can be gauged by comparing this solution to the homogeneous-fluid solution with the same topography. We find that both the Gulf Stream and the countercurrent are stronger than in the homogeneous-fluid case, and that the latter is concentrated in an $\epsilon^{1/2}$-thickness region of southward flow on the eastern edge of the Gulf Stream.

2. The two-layer model

We regard the ocean as a fluid composed of two immiscible layers with different, constant mass densities, bounded by a rigid lid at $z = 0$ and a bottom at $z = -H(x, y)$ (Fig. 1). The ocean depth goes smoothly to zero at the coastlines, and the front separating the layers with different densities can intersect the ocean surface or bottom. The governing form of the planetary geostrophic equations is (in dimensional form):

$$\begin{aligned} \mathbf{f} \times \mathbf{u}_1 &= -\nabla \phi_s - \epsilon \mathbf{u}_1 \\ \mathbf{f} \times \mathbf{u}_2 &= -\nabla \phi_s + g' \nabla h - \epsilon \mathbf{u}_2 \\ \frac{\partial h_i}{\partial t} + \nabla \cdot [\mathbf{u}_i h_i] &= 0. \end{aligned} \tag{2.1}$$

Here, $h_1 \equiv h$ is the vertical thickness of the top layer, h_2 the thickness of the bottom layer, $\mathbf{u}_i \equiv (u_i, v_i)$ are the corresponding horizontal velocities, ϕ_s is the pressure (divided by a constant representative density) at the surface, $\mathbf{f} = \beta y \, \mathbf{k}$, and g' is the reduced gravity. The wind forcing has been temporarily omitted. Since $h_1 + h_2 = H$, we must have

$$\nabla \cdot [h_1 \mathbf{u}_1 + h_2 \mathbf{u}_2] = 0. \tag{2.2}$$

Hence

$$h_1\mathbf{u}_1 + h_2\mathbf{u}_2 = \mathbf{k} \times \nabla\psi \tag{2.3}$$

where ψ is the transport streamfunction. From (2.1a,b) we also have

$$\mathbf{f} \times (\mathbf{u}_1 - \mathbf{u}_2) = -g'\nabla h - \epsilon(\mathbf{u}_1 - \mathbf{u}_2). \tag{2.4}$$

Using (2.3) and (2.4), we can write the horizontal velocities solely in terms of ψ and h. Assuming $f \gg \epsilon$, we obtain

$$\begin{aligned} \mathbf{u}_1 &= \frac{1}{H}\mathbf{k} \times \nabla\psi + \frac{g'}{f}\frac{h_2}{H}\mathbf{k} \times \nabla h - \epsilon\frac{g'}{f^2}\frac{h_2}{H}\nabla h \\ \mathbf{u}_2 &= \frac{1}{H}\mathbf{k} \times \nabla\psi - \frac{g'}{f}\frac{h_1}{H}\mathbf{k} \times \nabla h + \epsilon\frac{g'}{f^2}\frac{h_1}{H}\nabla h \end{aligned} \tag{2.5}$$

where, again, $h = h_1 = H - h_2$. The curl of the vertically-averaged momentum equation then yields the streamfunction equation,

$$J\left(\frac{f}{H}, \psi\right) + J\left(\frac{1}{2}g'h^2, \frac{1}{H}\right) = \nabla \cdot \left(\frac{\epsilon}{H}\nabla\psi\right) \tag{2.6}$$

where $J(A, B) \equiv A_xB_y - A_yB_x$ is the Jacobian. For the thermocline depth h, we may use the upper-layer mass conservation equation (2.1c). After substitutions from (2.5a), it takes the form

$$\frac{\partial h}{\partial t} + J\left(\psi, \frac{h}{H}\right) + J\left(g'h, \frac{h}{f}\left(1 - \frac{h}{H}\right)\right) = \nabla \cdot \left[\epsilon\frac{g'h}{f^2}\left(1 - \frac{h}{H}\right)\nabla h\right]. \tag{2.7}$$

Eqs. (2.6, 2.7) are the basic equations of the two-layer planetary geostrophic model. We can regard (2.6) as a generalization of Stommel's (1948) equation for the vertically-averaged vorticity, and (2.7) as an "internal Rossby wave" equation.

Numerical experiments (Salmon, 1990) with the continuously stratified form (1.1) of the planetary geostrophic equations have shown that the solutions always approach a steady state. We therefore seek steady solutions of (2.6, 2.7). It is convenient to rewrite the steady form of (2.6, 2.7) in nondimensional variables. Scaling x and y by L (the ocean basin size), h_i and H by H_0 (a representative abyssal depth), ψ by H_0LU, f by βL; and choosing the velocity scale $U = g'H_0\beta^{-1}L^{-2}$ to be the same as the propagation velocity of long Rossby waves, we obtain the nondimensional equations

$$J\left(\frac{f}{H}, \psi\right) + J\left(\frac{1}{2}h^2, \frac{1}{H}\right) = \nabla \cdot \left(\frac{\epsilon}{H}\nabla\psi\right) \tag{2.8}$$

and

$$J\left(\psi, \frac{h}{H}\right) + J\left(h, \frac{h}{f}\left(1 - \frac{h}{H}\right)\right) = \nabla \cdot \left[\epsilon \frac{h}{f^2}\left(1 - \frac{h}{H}\right)\nabla h\right] \tag{2.9}$$

where now $f = y$ and ϵ is the dimensional friction coefficient divided by βL. The boundary conditions on (2.8) are $\psi = 0$ at coastlines. Additional boundary conditions apply along the lines of intersection between the thermocline $z = -h$ and the ocean surface $z = 0$ or bottom $z = -H$. At the surface intersections (which we will call outcrops) the boundary condition is that the upper-layer velocity must (in steady state) be parallel to the outcrop, that is

$$\mathbf{u}_1 \cdot \nabla h = 0 \qquad at \qquad h = 0. \tag{2.10}$$

Substituting from (2.5a), (2.10) becomes

$$\frac{1}{H} J(\psi, h) = \frac{\epsilon}{f^2} \nabla h \cdot \nabla h \qquad at \qquad h = 0. \tag{2.11}$$

The boundary condition (2.11) can also be obtained by "evaluating" (2.9) at $h = 0$, but the separate, physical justification of (2.11) given here is really required; there is no fundamental reason why (2.9) should hold *at* the outcrop. If the thermocline intersects the bottom boundary, then the appropriate boundary condition is that the *lower* layer velocity be parallel to the line of intersection. However, only surface intersections will be considered in this paper.

3. Homogeneous flow

We consider first the case of an homogeneous ocean, for which the general equations (2.8, 2.9) (but now including wind-forcing) reduce to

$$J\left(\frac{f}{H}, \psi\right) = \nabla \cdot \left(\frac{\epsilon}{H} \nabla \psi\right) - W \tag{3.1}$$

with the boundary condition $\psi = 0$ at coastlines. We will assume that W, the prescribed wind-stress curl, is important only in the mid-ocean. Our purpose is to demonstrate the dramatic difference between a typical analytical solution of (3.1) along a western boundary stretching infinitely in the northward direction and the corresponding solution in a more realistic ocean with finite dimensions. We suppose that $H = H(x)$, assume that ϵ is small, neglect the frictional force in the x-direction in the usual way, and seek a solution in the form $\psi(x, y) = y\Psi(x)$. Then, also neglecting

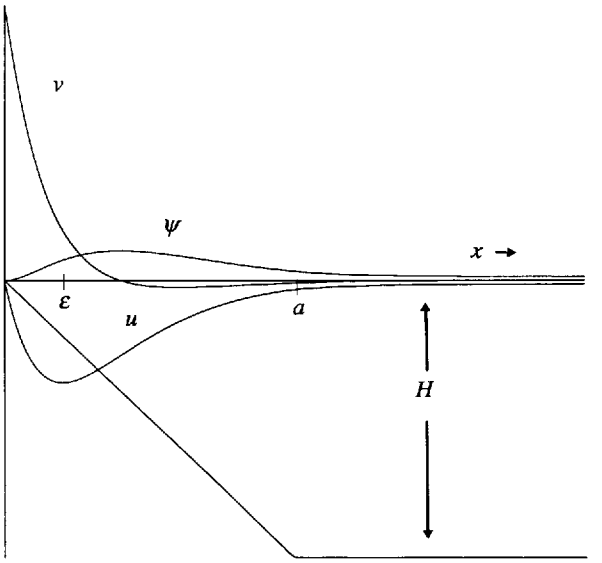

Figure 2. The eastward velocity u, northward velocity v, and transport streamfunction ψ according to the solution (3.4–6) for homogeneous flow in an ocean of depth H with a uniform continental slope of width a. The friction coefficient $\epsilon = .2a$. The flow is driven by an impinging eastward velocity at large x.

W in the western boundary region, (3.1) becomes an ordinary differential equation,

$$\epsilon \frac{d}{dx}\left(\frac{1}{H}\frac{d\Psi}{dx}\right) + \frac{1}{H}\frac{d\Psi}{dx} + \frac{H_x}{H^2}\Psi = 0 \tag{3.2}$$

with boundary condition $\Psi(0) = 0$. To facilitate analytical solution, we suppose that the ocean depth takes the simple form

$$H(x) = \begin{cases} sx, & 0 < x < a = 1/s \\ 1, & a < x \end{cases} \tag{3.3}$$

sketched in Figure 2. The uniform continental slope has constant width a. Then, omitting easy steps, we find that

$$\psi = \begin{cases} -\frac{1}{2}\frac{u_\infty s}{\epsilon} x^2 y\, e^{-(x-a)/\epsilon}, & 0 < x < a \\ -u_\infty y - \frac{1}{2}u_\infty\left(\frac{a}{\epsilon} - 2\right) y\, e^{-(x-a)/\epsilon}, & a < x. \end{cases} \tag{3.4}$$

The constant u_∞, which is the interior eastward velocity at large x, represents the effect of distant wind forcing in driving the boundary current along the sloping

western boundary. The corresponding velocity field,

$$\left.\begin{aligned} u &= \frac{1}{2}u_\infty \frac{x}{\epsilon} e^{-(x-a)/\epsilon} \\ v &= \frac{1}{2}\frac{u_\infty}{\epsilon} y\left[\frac{x}{\epsilon} - 2\right] e^{-(x-a)/\epsilon} \\ w &= \frac{1}{2}\frac{u_\infty}{\epsilon} z e^{-(x-a)/\epsilon} \end{aligned}\right\} 0 < x < a \tag{3.5}$$

and

$$\left.\begin{aligned} u &= u_\infty + \frac{1}{2}u_\infty\left(\frac{a}{\epsilon} - 2\right) e^{-(x-a)/\epsilon} \\ v &= \frac{1}{2}\frac{u_\infty}{\epsilon} y\left(\frac{a}{\epsilon} - 2\right) e^{-(x-a)/\epsilon} \\ w &= 0 \end{aligned}\right\} a < x \tag{3.6}$$

is shown in Figure 2 for the case of negative u_∞ (interior flow impinging on the coast) and $\epsilon = .2a$. The flow is northward west of $x = 2\epsilon$ with maximum velocity at the coast, where $H = 0$; the northward transport Hv reaches its maximum at $x = .59\epsilon$. To the east of $x = 2\epsilon$ lies a southward countercurrent. This countercurrent results from the tendency of fluid columns moving up the slope to conserve their potential vorticity, and in the limit $\epsilon \to 0$ its total transport approaches that of the northward flow (for reasons seen more clearly in the next example.) However, as $\epsilon \to 0$, both the boundary current and the countercurrent are squeezed into the corner at $x = 0$. Except for the countercurrent, the solution (3.4–6) resembles the classical theories of Stommel (1948) and Munk (1950). However, as we see next, this resemblance is an artificial consequence of the infinite horizontal geometry.

Consider next an ocean with the same continental slope near $x = 0$, but with northern and southern boundaries, as sketched in Figure 3. The southern boundary lies north of the equator at $y = 0$. In a notation that will also be useful later, we rewrite (3.1) in the advection-diffusion form

$$\mathbf{v}_{[f/H]} \cdot \nabla\psi = \nabla \cdot \left(\frac{\epsilon}{H}\nabla\psi\right) - W \tag{3.7}$$

where

$$\mathbf{v}_{[\mu]} \equiv \mathbf{k} \times \nabla\mu \tag{3.8}$$

is the "velocity field" with streamfunction $\mu(x, y)$. The arrows in Figure 3 indicate the direction of the $\mathbf{v}_{[f/H]}$ "flow." This "flow" enters the ocean basin at the eastern boundary, and at the northern boundary on the continental slope; it exits the basin

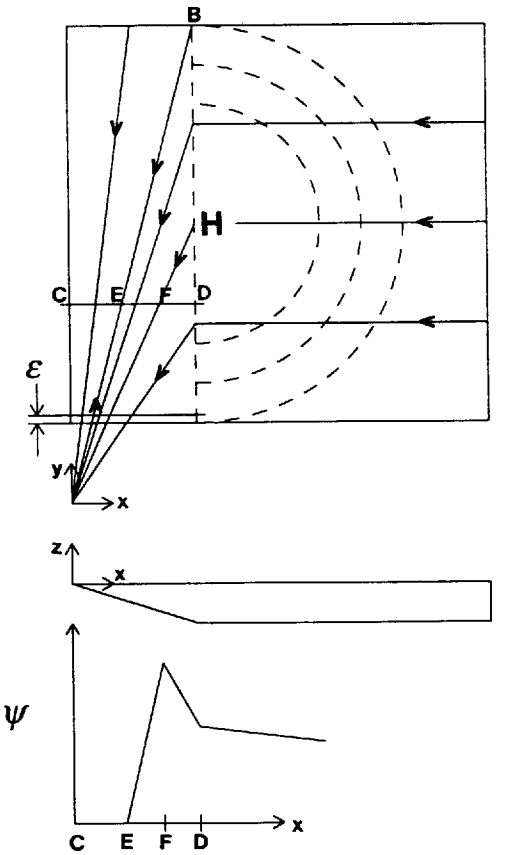

Figure 3. An homogeneous ocean with a continental slope along the western boundary. The arrows indicate the direction in which information flows along lines of constant f/H. The curved dashed lines are lines of constant transport streamfunction ψ in the interior ocean, assuming the standard subtropical wind gyre. On the continental slope, ψ is constant along lines of constant f/H, and frictional effects are confined to the southwestern boundary layer of thickness ϵ. The lower graph shows ψ along the section CD.

through the southern boundary on the continental slope, where (as at all boundaries) ψ must be zero. In the limit $\epsilon \to 0$, friction is important only in an ϵ-thickness boundary layer in this region of exiting "flow."

Now, suppose that the wind curl W is negative over the interior ocean (corresponding to the standard subtropical wind gyre) and zero at the north and south boundaries (to avoid an uninformative discussion of the boundary layers there). Then the mid-ocean $\psi(x, y)$ takes the form contoured by the dashed lines in Figure 3, with the maximum streamfunction at midlatitude and at the foot of the continental slope, where indicated by the "H." Suppose again that the wind curl is negligible over the continental slope, either because W actually vanishes there, or (more realisti-

cally) because the larger fluid velocities over the slope render it insignificant; this assumption is easily relaxed. Then outside the southern boundary layer, lines of constant ψ coincide with lines of constant f/H on the continental slope. On the f/H lines that originate at the northern boundary, ψ must be zero; thus the fluid is motionless in the region west of line AB in Figure 3. On the f/H lines that originate at the eastern boundary, the streamfunction on the continental slope has the same value as at the foot of the slope; that is

$$\psi = \psi_0\left(\frac{y}{H}\right) \tag{3.9}$$

where $\psi_0(y)$ is the value of ψ at the foot of the continental slope, where the fluid depth $H = 1$.

Now consider a section CD across the continental slope, south of the maximum interior ψ at mid-latitude. Refer again to Figure 3. To the west of E, the intersection between AB and CD, ψ vanishes, as shown on the lower graph in Figure 3. Between E and F, the intersection between CD and the f/H-line on which the interior streamfunction is maximum, ψ increases to the maximum value in the basin, and the flow is strongly northward. Between F and D, ψ decreases to its (positive) interior value, and the flow is strongly southward. Thus, in contrast to (3.4–6), the maximum velocity occurs not at the coastline but at some distance offshore. Moreover, neither the velocity nor the width of the northward flowing current (between E and F) and the southward flowing countercurrent (between F and D) depend on ϵ. Friction is important only in the southwestern boundary layer, which is the source of all northward flow. In the limit $\epsilon \to 0$, the total Sverdrup transport of the entire subtropical gyre is carried southward by the countercurrent into this frictional boundary layer.

If the friction ϵ is increased, the boundary layer thickens, and the streamlines begin to reconnect on the continental slope. However, the flow described above is qualitatively unchanged. Nor are our conclusions sensitively dependent on the precise geometry of Figure 3. If, for example, the ocean basin had a continental slope at all boundaries, so that f/H-lines never intersect a boundary, but all traverse the southern continental slope (as in Fig. 4), then (assuming $\epsilon \to 0$) the effects of friction are swept even further "downstream" by the $\mathbf{v}_{[f/H]}$ "flow." However, the salient point remains: the western boundary current system is, asymptotically, *locally* independent of the friction, and the flow on the slope is solely determined by the bottom topography and by the interior streamfunction values built up by the wind forcing.

From the perspective of Figure 3, we can also easily understand the artificial dependence of the analytical solution (3.4–6) on the friction parameter ϵ. Imagine that the northern ocean boundary in Figure 3 is moved northward by an arbitrarily large amount. In that limit, characteristic lines originating on the eastern boundary at arbitrarily high latitude (and therefore, on the assumption of a uniform westward

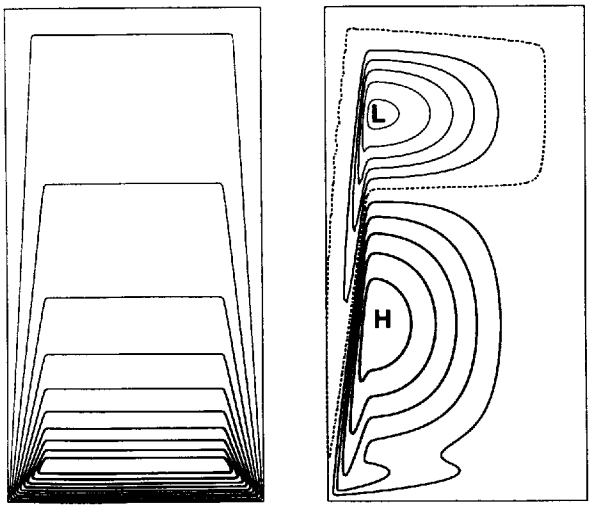

Figure 4. The transport streamfunction ψ (right) satisfying the Eq. (3.1), with $\epsilon = .01$, for homogeneous wind-driven flow in an ocean with uniform continental slopes at all boundaries, so that the H/f lines are as shown on the left. The wind curl, which is nonzero only in the flat-bottomed interior ocean, corresponds to the standard two-gyre case.

interior flow, carrying arbitrarily large values of ψ) pass arbitrarily close to the western coastline, where of course $\psi = 0$. The resulting arbitrarily large gradient of ψ at $x = 0$ makes friction important there, no matter how small ϵ.

Figure 4 shows a numerical solution of (3.1) in an ocean with uniform slopes at all coasts, so that the H/f-lines are as shown on the left. The wind stress curl is nonzero only in the flat-bottomed interior ocean, where it corresponds to an anticyclonic subtropical gyre in the southern two-thirds of the interior, and a cyclonic subpolar gyre in the north. In the southern part of the western continental slope, the streamfunction resembles that described above, with a strong southward flow on the seaward side of the Gulf Stream. To the north, the low streamfunction values produced by the wind in the subpolar gyre are carried southwestward by the $\mathbf{v}_{[f/H]}$ "flow" along f/H-lines to produce a new region of southward flow between the inshore region of stagnant flow and the strong northward flow in the Gulf Stream. This southward flow corresponds to the southward flow observed west of the Gulf Stream in the Middle Atlantic Bight. (See, for example, the velocity sections near Cape Hatteras analyzed by Joyce *et al.* (1986).) A solution closely resembling that shown in Figures 3 and 4 was calculated by Holland (1967). See his Figure 17 and surrounding discussion.

Lee *et al.* (1990) and Leaman and Harris (1990) report observations of a very strong, deep southward flow east of the Bahamas at 26.5N. They estimate the average total transport at 30–35 Sverdrups, which is about equal to the total Sverdrup

transport of the entire subtropical wind gyre. Leaman and Harris note that this huge southward transport does not coincide with the deep western boundary current as defined by tracer data. This suggests that this southward flow may be fed from more southerly latitudes than the latter, in agreement with the explanation offered here. However, most of this southward flowing water is much colder than the water flowing through the Florida Straits, so that diabatic heating is required to complete the part of the circuit represented by the southwestern boundary layer in Figure 3. Of course, real bathymetry bears little resemblance to that sketched in Figure 3, but our reasoning does not depend on the exact form of the topography.

It thus appears that neither friction nor inertia may be required to explain some of the most prominent features of the flow along western boundaries. However, our reasoning seems to depend very strongly on the assumption of an homogeneous fluid, and even crude estimates of the Joint Effect of Baroclinicity (i.e. inhomogeneity) and Relief—the so-called JEBAR effect—suggest that second term in (2.8) is as important as any of the terms retained in (3.1). In the following two sections, we resolve this paradox with solutions of the general two-layer equations which, despite the leading-order importance of JEBAR, bear a surprising qualitative resemblance to the solutions for homogeneous flow.

4. General solution of the outer equations

We now consider the general two-layer equations (2.8, 2.9) on a western continental slope, again assuming that the local wind-forcing is unimportant. Our solutions will be driven by matching to a wind-driven interior ocean. We anticipate that, in the limit $\epsilon \to 0$, the frictional terms in (2.8, 2.9) are also unimportant except in narrow vertical layers on the boundaries or in the interior. To avoid confusing terminology, we call the regions of negligible friction "outer regions," and we call the frictional layers "inner regions," regardless of where they occur. We will find that the inner regions typically occur away from boundaries, but not primarily at outcrops.

In the outer regions, where friction is unimportant, the equations (2.8, 2.9) reduce to

$$J\left(\frac{f}{H}, \psi\right) + J\left(\frac{1}{2}h^2, \frac{1}{H}\right) = 0 \tag{4.1}$$

and

$$J\left(\psi, \frac{h}{H}\right) + J\left(h, \frac{h}{f}\left(1 - \frac{h}{H}\right)\right) = 0. \tag{4.2}$$

The general solution can be written in implicit form. We assume that $\nabla H \neq 0$; the easier case of constant depth will be considered in Section 5. The trick is to eliminate

f and H in favor of the potential vorticities

$$q_1 \equiv \frac{h}{f}, \qquad q_2 \equiv \frac{H-h}{f}. \tag{4.3}$$

Then the outer equations (4.1, 4.2) take the forms

$$J\left(\frac{1}{q_1+q_2}, \psi\right) + J\left(h, \frac{q_1}{q_1+q_2}\right) = 0 \tag{4.4}$$

and

$$J\left(\psi, \frac{q_1}{q_1+q_2}\right) + J\left(h, \frac{q_1 q_2}{q_1+q_2}\right) = 0. \tag{4.5}$$

Our definition of potential vorticity is the reciprocal of the usual one, but it is the more convenient here.

The solution proceeds easiest if we rewrite (4.4, 4.5) in the equivalent forms

$$J(\psi, q_1) + q_2 J(h, q_1) = 0 \tag{4.6}$$

and

$$J(\psi, q_2) - q_1 J(h, q_2) = 0. \tag{4.7}$$

Eqs. (4.6, 4.7) are the frictionless limits of the upper and lower layer potential vorticity equations. There are two cases to consider. In the first case,

$$\frac{\partial(q_1, q_2)}{\partial(x, y)} \neq 0. \tag{4.8}$$

If (4.8) holds, then we may take (q_1, q_2) as new independent variables. Dividing (4.6, 4.7) by the left-hand side of (4.8), we obtain

$$\frac{\partial \psi}{\partial q_2} + q_2 \frac{\partial h}{\partial q_2} = 0, \qquad \frac{\partial \psi}{\partial q_1} - q_1 \frac{\partial h}{\partial q_1} = 0. \tag{4.9}$$

Eliminating ψ from (4.9) yields

$$(q_1 + q_2) \frac{\partial^2 h}{\partial q_1 \partial q_2} = 0. \tag{4.10}$$

But since $q_1 + q_2 = H/f$ never vanishes, we must have

$$h = F'(q_1) + G'(q_2) \tag{4.11}$$

where F and G are arbitrary functions, and the primes, which denote differentiation,

are introduced for convenience. Substituting (4.11) back into (4.9), we easily obtain

$$\psi = q_1 F'(q_1) - F(q_1) - q_2 G'(q_2) + G(q_2) \tag{4.12}$$

(where arbitrary constants have been absorbed into F and G). It is easy to verify that (4.11, 4.12) satisfy (4.9) for any F and G.

In the second case,

$$\frac{\partial(q_1, q_2)}{\partial(x, y)} = 0. \tag{4.13}$$

We will see that (4.13) can be satisfied only if q_1 or q_2 is uniform. If (4.13) holds, then, by (4.3), h/f is constant on lines of constant H/f. That is,

$$\frac{h}{f} = E\left(\frac{H}{f}\right) \tag{4.14}$$

for some function E. We now regard ψ and

$$\Phi \equiv \frac{h}{H} \tag{4.15}$$

as the dependent variables, and regard H and

$$\alpha \equiv \frac{H}{f} \tag{4.16}$$

as new independent variables. Then, dividing our fundamental equations (4.1, 4.2) by

$$\frac{\partial(\alpha, H)}{\partial(x, y)} \tag{4.17}$$

we obtain the equivalent equations

$$\frac{\partial \psi}{\partial H} = -\alpha^2 \Phi \frac{\partial \Phi}{\partial \alpha} \tag{4.18}$$

and

$$\frac{\partial(\psi, \Phi)}{\partial(\alpha, H)} + \frac{\partial(H\Phi, \alpha\Phi(1 - \Phi))}{\partial(\alpha, H)} = 0. \tag{4.19}$$

But (4.14) implies that $\partial\Phi/\partial H = 0$, whereupon (4.18) integrates to

$$\psi = R(\alpha) - \alpha^2 H \Phi(\alpha) \frac{d\Phi}{d\alpha} \tag{4.20}$$

where R is an arbitrary function. Then, substituting (4.20) into our other fundamen-

tal equation (4.19), we obtain the ordinary differential equation

$$\alpha^2\Phi\left(\frac{d\Phi}{d\alpha}\right)^2 = \Phi\frac{d}{d\alpha}[\alpha\Phi(1-\Phi)] \tag{4.21}$$

for $\Phi(\alpha)$. The solutions of (4.21) are easily found to be

$$\Phi = const/\alpha \qquad \text{and} \qquad \Phi = 1 + const/\alpha. \tag{4.22}$$

In each of these two cases, the corresponding transport streamfunction is given by (4.20). Translating these two solutions into original notation, we obtain

$$\begin{cases} \psi = R_1\left(\dfrac{H}{f}\right) + Q_1^2 f \\ h = Q_1 f \end{cases} \tag{4.23}$$

and

$$\begin{cases} \psi = R_2\left(\dfrac{H}{f}\right) - Q_2 H + Q_2^2 f \\ h = H - Q_2 f \end{cases} \tag{4.24}$$

where R_i are arbitrary functions and Q_i are arbitrary constants. It is easy to verify that (4.23) and (4.24) are exact solutions of the fundamental outer equations (4.1, 4.2). In overall summary, the general solution of (4.1, 4.2) is (4.11, 4.12) or (4.23) or (4.24); the homogeneous-fluid solution corresponds to (4.23) with $Q_1 = 0$.

In comparison to (4.11, 4.12), the solutions (4.23) or (4.24) seem rather special, but they seem also to have a special significance. The solution (4.23) corresponds to a region of uniform upper-layer potential vorticity, $q_1 = Q_1$. Similarly (4.24) corresponds to a region of uniform lower-layer potential vorticity, $q_2 = Q_2$. In both of these solutions, the transport streamfunction contains an arbitrary function of H/f, and in this it resembles the solution for homogeneous flow (Section 3).

The contrast between (4.11, 4.12) and (4.23, 4.24) can be drawn further by writing the basic equations in characteristic form. The characteristic equations, which are most readily deduced from (4.9), are

$$q_1 = const \qquad \text{on} \qquad \frac{d\psi}{dh} = -q_2 \tag{4.25}$$

and

$$q_2 = const \qquad \text{on} \qquad \frac{d\psi}{dh} = q_1 \tag{4.26}$$

where we now regard ψ and h as independent variables. That is, q_1 is the Riemann invariant on characteristic lines of slope $-q_2$ (in the h-ψ plane), and q_2 is the

Riemann invariant on characteristic lines of slope q_1. However, it is not difficult to show that the characteristics defined by (4.25, 4.26) typically cross, producing shocks at which the solutions become multi-valued unless friction is readmitted to resolve the multivalued-ness. This situation simply corresponds to choices of F and G for which (4.11, 4.12) cannot be solved uniquely for h and ψ.

From this perspective, the special solutions (4.23) or (4.24) correspond to cases in which one of the two Riemann invariants is uniform, and, according to (4.25, 4.26), the other family of characteristics has a uniform slope so that no shocks can occur. Indeed, we see directly from (4.23, 4.24), that in the solutions with uniform q_1, $\psi - q_1^2 f$ is constant along lines of constant H/f; and in the solutions with uniform q_2, $\psi + q_2 H - q_2^2 f$ is constant along lines of constant H/f. In both of the solutions (4.23, 4.24), the characteristics are lines of constant H/f in ordinary physical space.

Regions in which one of two Riemann invariants is uniform play an important role in the theory of gas dynamics. In typical gas dynamics problems, the *same* Riemann invariant is uniform over the whole flow. However, the most oceanographically interesting solutions of (4.1, 4.2) seem to be those in which each of the two solutions (4.23) and (4.24) obtains over some region of the flow. Before constructing such solutions, we first show that the boundary between two such regions must itself be a line of constant H/f.

The latter statement follows from the general result that, in exactly hyperbolic systems, discontinuities can occur only at characteristics. However, it is illuminating to give a direct proof based upon the jump conditions at the lines separating regions in which distinct solutions of types (4.23) or (4.24) obtain. To obtain these jump conditions, we rewrite the general *frictional* equations (2.8, 2.9) in "flux form"

$$\nabla \cdot \mathbf{F}_1 = 0, \qquad \nabla \cdot \mathbf{F}_2 = 0 \tag{4.27}$$

where

$$\mathbf{F}_1 = \mathbf{v}_{[f/H]}\psi - \mathbf{v}_{[1/H]}\frac{1}{2}h^2 - \frac{\epsilon}{H}\nabla\psi \tag{4.28}$$

and

$$\mathbf{F}_2 = -\mathbf{v}_{[h/H]}\psi + \mathbf{v}_{[h]}\frac{h}{f}\left(1 - \frac{h}{H}\right) - \epsilon\frac{h}{f^2}\left(1 - \frac{h}{H}\right)\nabla h \tag{4.29}$$

where $\mathbf{v}_{[\mu]}$ is again defined by (3.8) as the "velocity field" corresponding to the streamfunction μ. Now let C be a curve, with normal $\mathbf{n}$, separating regions with distinct outer solutions of the types (4.23) or (4.24), at which the outer solutions or their derivatives are discontinuous. A thin inner region, in which the ϵ-terms become important, must exist along C to join the discontinuous outer solutions smoothly together. By the usual argument, the normal components of $\mathbf{F}_i$ must be constant

across this thin inner region; this leads to the jump conditions

$$\Delta \left[\mathbf{v}_{[f/H]}\psi - \mathbf{v}_{[1/H]} \frac{1}{2} h^2\right] \cdot \mathbf{n} = 0 \tag{4.30}$$

and

$$\Delta\left[-\mathbf{v}_{[h/H]}\psi + \mathbf{v}_{[h]} \frac{h}{f}\left(1 - \frac{h}{H}\right)\right] \cdot \mathbf{n} = 0 \tag{4.31}$$

where Δ denotes the jump in the outer solutions. There are, of course, no jumps in f or H. Let s be the distance along C. Then (4.30) implies that

$$\frac{d}{ds}\left(\frac{f}{H}\right)\Delta\psi = \frac{d}{ds}\left(\frac{1}{H}\right)\Delta\left(\frac{1}{2}h^2\right) \tag{4.32}$$

or, in other notation,

$$\frac{d\alpha}{dH}\Delta\psi = \alpha^2\Delta\left(\frac{1}{2}\Phi^2\right) \tag{4.33}$$

where $d\alpha/dH$ is measured along C. Now, in all solutions of the types (4.23) or (4.24), the right-hand side of (4.33) depends only on α (and not on H). But the left-hand side of (4.33) is H-independent only if $d\alpha/dH = 0$; that is, C must be a line of constant H/f. It then follows from (4.32) that $\Delta h = 0$; that is, the outer thermocline depths must be continuous at C. (The latter conclusion does not apply to flow over a flat bottom, where $dH^{-1}/ds = 0$ in Eq. 4.32.) By similar steps, the second jump condition (4.31) can be written

$$\Delta\left[\psi \frac{d\Phi}{ds}\right] = \Delta\left[\alpha\Phi(1 - \Phi)\frac{d}{ds}(H\Phi)\right]. \tag{4.34}$$

The right-hand side vanishes, since neither Φ nor its derivative along C jumps. The left-hand side vanishes because $d\Phi/ds = 0$ along a line of constant H/f in either of the two outer solutions (4.23) or (4.24).

In the next section we construct a theory of the Gulf Stream based upon the outer solutions (4.23, 4.24) and the information obtained above from the analysis of the jump conditions. The complete theory requires an inner-region analysis, but the physical role of the inner region will be obvious from the jumps in the outer solutions.

In retrospect, it is somewhat surprising that the nonlinear equations (4.1, 4.2) can be completely solved. However, (4.1, 4.2) can be transformed into *quasi-linear* equations by considering α and Φ, defined by (4.15) and (4.16), as functions of h and ψ. Then (4.1, 4.2) are equivalent to

$$\frac{\partial\alpha}{\partial h} = \alpha^2 \frac{\partial\Phi}{\partial\psi} \tag{4.35}$$

and

$$\frac{\partial \Phi}{\partial h} = \Phi(1 - \Phi)\frac{\partial \alpha}{\partial \psi} + \alpha(1-2\Phi)\frac{\partial \Phi}{\partial \psi}. \tag{4.36}$$

Standard methods lead to the characteristic equations (4.25, 4.26) (but without assuming that q_1, q_2 comprise good coordinates) and—eventually—to the other results quoted above. However, the line of reasoning followed above seems to be more economical.

5. Gulf Stream solution

We now consider an ocean with the same geometry as in Section 3, and again assume that the direct effects of wind-forcing can be neglected on the continental slope. In the mid-ocean, where $H = 1$, the general equations (2.8, 2.9) reduce to

$$-\frac{\partial \psi}{\partial x} = \epsilon \nabla^2 \psi + W_\psi \tag{5.1}$$

and

$$J(\psi, h) - \frac{1}{f^2}h(1 - h)h_x = \nabla \cdot \left[\epsilon \frac{h}{f^2}(1 - h)\nabla h\right] + W_h \tag{5.2}$$

which are the equations considered by Dewar (1991). Here W_ψ and W_h are the wind-forcing on the barotropic and baroclinic modes; their precise forms do not concern us. The *outer* (i.e. $\epsilon \to 0$) solution of (5.1) can have jumps in ψ across latitude lines, but these jumps, starting at the eastern boundary region, would be considerably smoothed as x approaches the western boundary region, by even a relatively small friction ϵ in the parabolic equation (5.1). Therefore, following Dewar, we assume that the mid-ocean transport streamfunction is smooth. The precise form of $\psi(x, y)$ depends not only on the wind forcing term W_ψ, but also on the matching conditions at the foot of the eastern continental slope.

With given, smooth $\psi(x, y)$, the mid-ocean thermocline depth h is determined from (5.2). However, as emphasized by Dewar, the outer solutions of (5.2) can then still have jumps in h along lines determined by the jump conditions (4.34). In this paper, we are interested in the structure of the solutions on the western continental slope, and we take the interior fields to be given (and to resemble those observed). However, since the analysis in Section 4 has shown that outer solutions of the types (4.23) or (4.24) over sloping topography cannot exhibit jumps in h, and because these must match to the mid-ocean solutions, we will assume that *both* ψ and h contain no jumps in the mid-ocean. We also note that no jumps in h seem to occur in numerical solutions of the general, continuously stratified planetary geostrophic equations (1.1) (Salmon, 1990).

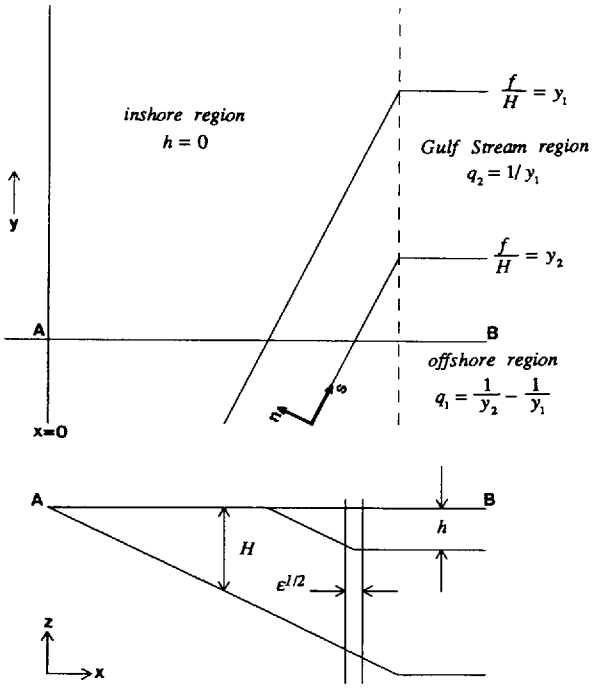

Figure 5. Above: Plan view of the Gulf Stream solution (5.3–5). The two lines of constant f/H separate the Gulf Stream region, $y_2 < f/H < y_1$, from the northward region of vanishing upper-layer thickness and the southward region of uniform upper-layer potential vorticity. The coordinates n and s are boundary-layer coordinates for the inner region at $f/H = y_2$. Below: The section AB across the continental slope, showing the $\epsilon^{1/2}$-thickness inner region of concentrated southward flow at the eastern edge of the Gulf Stream.

On the western continental slope, our solution consists of three regions:

(a) a northern and *in-shore region* $\alpha \equiv H/f < \alpha_1$, in which the upper-layer thickness is zero;

(b) a *Gulf Stream region* $\alpha_1 < \alpha < \alpha_2$, in which the lower-layer potential vorticity is uniform, and the outer solution takes the form (4.24); and

(c) *an off-shore region* $\alpha_2 < \alpha$, in which the upper-layer potential vorticity is uniform, and the outer solution takes the form (4.23).

Refer to Figure 5. Thus, in the Gulf Stream region, the thermocline has the same shape as the ocean bottom in constant-latitude sections, and shoals to the north. The assumption of an offshore region of constant upper-layer potential vorticity is based on the remarkable observation (apparently first made by Stommel (1965, p. 112) and still, in my opinion, not convincingly explained) that the depth of (say) the ten degree

isotherm is proportional to latitude in a large region of the subtropical North Atlantic.

The boundaries between the three regions reach the mid-ocean at the latitudes y_1 and y_2 in Figure 5. Since $h = 0$ at $\alpha = \alpha_1$, the uniform lower-layer potential vorticity in the Gulf Stream region must, by (4.24), be $Q_2 = \alpha_1 = y_1^{-1}$. And since there are no jumps in h at $\alpha = \alpha_2$, we must have $Q_1 + Q_2 = \alpha_2 = y_2^{-1}$ in (4.23). Then, choosing the arbitrary functions of H/f that appear in (4.23, 4.24) to match the prescribed mid-ocean transport streamfunction $\psi_0(y)$ at the foot of the continental slope, we obtain the complete set of outer solutions

$$\begin{cases} \psi = \psi_0\left(\dfrac{y}{H}\right) & \textit{in the inshore region } \left(\dfrac{H}{y} < \dfrac{1}{y_1}\right) \\ h = 0 \end{cases} \tag{5.3}$$

$$\begin{cases} \psi = \psi_0\left(\dfrac{y}{H}\right) + \dfrac{(1-H)}{y_1} + \dfrac{y}{y_1^2}\left(\dfrac{H-1}{H}\right) & \textit{in the Gulf Stream region } \left(\dfrac{1}{y_1} < \dfrac{H}{y} < \dfrac{1}{y_2}\right) \\ h = H - \dfrac{y}{y_1} \end{cases} \tag{5.4}$$

$$\begin{cases} \psi = \psi_0\left(\dfrac{y}{H}\right) + y\left[\dfrac{(y_1 - y_2)}{y_1 y_2}\right]^2 \dfrac{(H-1)}{H} & \textit{in the offshore region } \left(\dfrac{1}{y_2} < \dfrac{H}{y}\right) \\ h = \dfrac{(y_1 - y_2)}{y_1 y_2} y\,. \end{cases} \tag{5.5}$$

Here, $\psi_0(y/H)$ is the *same* transport streamfunction obtained in Section 3 for the case of homogeneous fluid. The non-ψ_0 terms in (5.3–5) thus represent the effects of baroclinicity and bottom topography.

According to the outer solutions (5.3–5), there are (as required by the jump conditions) no jumps in h anywhere in the flow, and the only jump in ψ occurs at the boundary $f/H = y_2$ between the Gulf Stream and the offshore region of uniform upper-layer potential vorticity. At this boundary, an inner region must exist to resolve the discontinuity in ψ (and, less importantly, in the normal derivative of h), and the complete solution requires an analysis of this inner region. A second, relatively unimportant, inner region is present at the western boundary of the Gulf Stream, where it is required to resolve a discontinuity in the normal derivative of ψ. However, the most important properties of the solution follow directly from the outer solutions (5.3–5).

The constants y_1 and y_2 are arbitrary. However, analytical and numerical solutions of the continuously stratified planetary geostrophic equations for the mid-ocean (Salmon, 1990; Salmon and Hollerbach, 1991) suggest that the main thermocline occurs only where the surface Ekman pumping velocity is downward. This, in turn, suggests that the outcropping line in mid-ocean coincides with the line of zero

wind-stress curl, and that, in present context, y_1 should be the latitude at which this zero-curl line reaches the foot of the continental slope. The latitude y_2 can then be chosen to match the mid-ocean maximum thermocline depth

$$h(y_2) = \frac{y_1 - y_2}{y_1} \tag{5.6}$$

to that observed (about .2 in nondimensional units); this gives $y_2 = .8y_1$. On the other hand, we might choose y_2 to match the Gulf Stream width, $y_1 - y_2$, to that observed (about 100 km); that gives $y_2 = .95y_1$.

From (5.3–5) we see that the *total* long-shore transport on the shelf, between the outcrop and the foot of the continental slope, is unchanged by the effects of baroclinicity and relief. However, the northward transport of the Gulf Stream is increased by an amount

$$\frac{y_1 - y_2}{y_1^2}\left[1 - \frac{y}{y_2}\right] \tag{5.7}$$

which is positive at all latitudes south of the latitude y_2 at which the eastern edge of the Gulf Stream reaches the abyss. The northward transport in the offshore region, between the eastern edge of the Gulf Stream and the foot of the continental slope, also increases, by the amount

$$\left[\frac{y_1 - y_2}{y_1 y_2}\right]^2 [y_2 - y]. \tag{5.8}$$

However, these two increases are cancelled by the jump in ψ at the boundary between the Gulf Stream and the offshore region. This jump (from west to east) is negative, and represents a southward flowing countercurrent with transport equal to the sum of (5.7) and (5.8). Thus, overall, the effects of baroclinicity and relief are to increase the transport of *both* the Gulf Stream *and* the southward flow to its east, but to concentrate the latter increase in a strong, thin countercurrent at the eastern edge of the Gulf Stream. In dimensional units, the increase (5.7) in Gulf Stream transport is

$$\Delta\psi = \frac{g'H_0^2}{\beta}\frac{(y_1 - y_2)}{y_1^2}\left(1 - \frac{y}{y_2}\right). \tag{5.9}$$

For $g' = 10^{-2}$ m sec^{-2}, $H_0 = 4$ km, $\beta = 10^{-11}$ m^{-1} sec^{-1}, $y_2 = .95y_1$, $y_1 = 4000$ km, and (say) $y = .5y_2$, (5.9) predicts a transport increase of about 100 Sverdrups, but this estimate depends sensitively on several factors.

Holland (1973) compared numerical solutions of the primitive equations in a square ocean with a western continental slope. He found that solutions with nonuniform temperature showed a strong recirculation over the slope, with a total

transport more than twice as large as the Sverdrup transport. He concluded that "when bottom topography and baroclinic effects are included in a wind-driven ocean model, the western boundary current can have a transport larger than that predicted from the wind stress distribution, even when the nonlinear advective terms [i.e. inertia] are ignored." Theoretical estimates by Huthnance (1984) also anticipate that baroclinicity and relief increase the transport on continental shelves.

The solution sketched in Figure 5 resembles the velocity sections inferred by Joyce *et al.* (1986) from acoustic and CTD data at locations just before—and just after—the Gulf Stream leaves the continental slope near Cape Hatteras. The upstream section (their Figure 4a) shows a region of weak, depth-independent, southward flow near the coast (as anticipated in Section 3), a Gulf Stream region in which the isopycnals parallel the sloping bottom, and an offshore region in which the thermocline depth is more nearly constant. Between the latter two regions is a relatively thin (60 km) region of strong southward flow, corresponding to the inner-region countercurrent in the solution proposed here. This southward flow is strongest near the bottom, where it would be called the Deep Western Boundary Current. In the conventional explanation, the Deep Western Boundary Current is driven by the interior upwelling required to compensate sinking at high latitudes. However, according to the theory offered here, this current would be present east of the Gulf Stream even if thermohaline forcing were absent altogether. The observed Deep Western Boundary Current may be playing a dual role.

Now consider the inner region at the boundary $f/H = y_2$ between the Gulf Stream and the offshore region. Let s be the distance downstream along this line, and let n be the distance in the shoreward normal direction, as shown on Figure 5. The inner-region approximation to (2.8) is

$$-\frac{\partial}{\partial n}\left(\frac{f}{H}\right)\frac{\partial \psi}{\partial s} = \frac{\epsilon}{H}\frac{\partial^2 \psi}{\partial n^2} - h\frac{\partial\left(h, \frac{1}{H}\right)}{\partial(s, n)} \tag{5.10}$$

because $\partial(f/H)/\partial s = 0$. Eq. (5.10) is a parabolic ("heat") equation for ψ in which "time" runs in the negative-s direction. The parabolic character of (5.10) depends critically on the orientation of the inner region; if the inner region were not parallel to a line of H/f then a term proportional to $\partial\psi/\partial n$ would also occur on the left-hand side of (5.10). The last term in (5.10)—the JEBAR term—is a "source" that vanishes in mid-ocean (where (5.10) reduces to (5.1)) but is nonzero on the continental slope. According to the outer solutions, this "source" has different values on the two sides of the inner region, and this difference (which is of course smoothed by the inner-region) produces the n-direction change in ψ needed to match the discontinuous outer solutions. Since only the normal derivative of h—and not h itself—jumps across the inner region, the JEBAR "source" in (5.10) has the same size as in the outer regions. It then follows from (5.10) that the inner region thickness must be $\epsilon^{1/2}$.

The ϵ determined by matching this thickness to the observed countercurrent thickness (60 km) is much smaller than that obtained by requiring the conventional ϵ-thickness Stommel boundary layer to match the observed Gulf Stream width (100 km.)

6. Speculation

If one accepts that the western continental slope region is one in which the local wind is relatively unimportant, and that dissipation terms are also unimportant outside thin inner regions, then the outer-region solutions must take the form (4.11, 4.12), (4.23), or (4.24). In this paper I have suggested that realistic solutions are combinations of the latter two (uniform potential vorticity) types, and that a simple solution, consisting of only three regions, resembles reality. But why should solutions of the more general form (4.11, 4.12) not be realized? And, in solutions of the form (4.23) or (4.24), what determines the number of uniform-potential-vorticity regions that actually occur? These questions can be answered only in the context of a whole-basin, time-dependent theory whose first task is to explain why stable *steady* solutions exist at all. However, I conjecture that solutions of the form (4.11, 4.12) (with shocks fitted as necessary!) will turn out to be generally unstable, and that the number of required uniform-potential-vorticity regions in solutions of the form (4.23) or (4.24) will increase with the complexity of the bottom topography. Although all of our outer solutions hold for arbitrary $H(x, y)$, the time-dependent equations ultimately decide between the myriad of possible patchings. The specific three-region solution given in Section 5 may have meaning for the relatively smooth topography along the mid-Atlantic coast, but many more outer regions may be required on the much more rugged topography southeast of Florida. Even if one accepts the three-region solution of Section 5, a full-basin theory is evidently needed. Although the solution in Section 5 matches an arbitrary interior *barotropic* flow $\psi_0(y)$, it requires that the interior *baroclinic* flow be one of uniform upper-layer potential vorticity. And, although this seems to be what is observed, the whole explanation is—at this point—frustratingly circular. A completely deductive theory is a very considerable challenge, but we can perhaps find some consolation in the prospect that such a theory need not necessarily include inertia.

Despite these many caveats, I find it very tantalizing that the solution proposed in Section 5 is one in which the potential vorticity of the ocean is—in some sense—as uniform as possible. The upper- and lower-layer potential vorticities cannot, of course, both be uniform in the same region. The principle that seems to be followed is that the upper (most active?) layer aquires a uniform potential vorticity, except in regions of large bottom slope; there, the lower-layer potential vorticity is uniform.

The idea of uniform potential vorticity has gained great currency in recent years. Uniform potential vorticity states have been attributed to the mixing of water particles in physical space (Rhines and Young, 1982) and to the mixing of system

states in phase space (e.g. Salmon, 1982). However, neither explanation applies satisfactorily to the planetary geostrophic equations, which, according to numerical experiments, slowly evolve to *steady* final states, in which the eddy-fluxes vanish. If steady final states like (5.3–5) are in fact realized by numerical solutions of the planetary geostrophic equations, then a new, essentially deterministic explanation must be sought, based more closely on the mathematical properties of (1.1).

Acknowledgments. It is a pleasure to thank Dr. Philip S. Bogden for long and illuminating conversations about the North Atlantic circulation. George E. Backus contributed an essential step to the analysis in Section 4. Thanks also to Donald B. Olson and George Veronis for their valuable comments. This work was supported by the National Science Foundation (OCE-8901720).

REFERENCES

Dewar, W. K. 1991. Arrested fronts. J. Mar. Res., *49,* 21–52.

Holland, W. R. 1967. On the wind-driven circulation in an ocean with bottom topography. Tellus, *19,* 582–599.

—— 1973. Baroclinic and topographic influences on the transport in western boundary currents. Geophys. Fluid Dyn., *4,* 187–210.

Huthnance, J. M. 1984. Slope currents and JEBAR. J. Phys. Oceanogr., *14,* 795–810.

Joyce, T. M., C. Wunsch and S. D. Pierce. 1986. Synoptic Gulf Stream velocity profiles through simultaneous inversion of hydrographic and acoustic Doppler data. J. Geophys. Res., *91,* C6, 7573–7585.

Killworth, P. D. 1983. Some thoughts on the thermocline equations. Ocean Model., *48,* 1–5.

Leaman, K. D. and J. E. Harris. 1990. On the average absolute transport of the deep western boundary currents east of Abaco Island, the Bahamas. J. Phys. Oceanogr., *20,* 467–475.

Lee, T. N., W. Johns, F. Schott and R. Zantopp. 1990. Western boundary current structure and variability east of Abaco, Bahamas at 26.5N. J. Phys. Oceanogr., *20,* 446–466.

Munk, W. H. 1950. On the wind-driven ocean circulation. J. Meteor., *7,* 79–93.

Pedlosky, J. 1968. An overlooked aspect of the wind-driven oceanic circulation. J. Fluid Mech., *32,* 809–821.

—— 1969. Linear theory of the circulation of a stratified ocean. J. Fluid Mech., *35,* 185–205.

Rhines, P. B. and W. R. Young. 1982. Homogenization of potential vorticity in planetary gyres. J. Fluid Mech., *122,* 347–367.

Salmon, R. 1982. The shape of the main thermocline. J. Phys. Oceanogr., *12,* 1458–1479.

—— 1986. A simplified linear ocean circulation theory. J. Mar. Res., *44,* 695–711.

—— 1990. The thermocline as an "internal boundary layer." J. Mar. Res., *48,* 437–469.

Salmon, R. and R. Hollerbach. 1991. Similarity solutions of the thermocline equations. J. Mar. Res., *49,* 249–280.

Stommel, H. 1948. The western intensification of wind-driven ocean currents. Am. Geophys. Union Trans., *29,* 202–206.

—— 1965. The Gulf Stream. (second edition) University of California Press, 248 pp.

Received: *3 February, 1992;* revised: *20 May, 1992.*